Am J Physiol Heart Circ Physiol 294: H2646–H2652, 2008.
First published April 11, 2008; doi:10.1152/ajpheart.00291.2008.

VEGF promotes vascular sympathetic innervation

Stephen B. Marko and Deborah H. Damon

Department of Pharmacology, University of Vermont, Burlington, Vermont

Submitted 17 March 2008; accepted in final form 2 April 2008

Marko SB, Damon DH. VEGF promotes vascular sympathetic innervation. *Am J Physiol Heart Circ Physiol* 294: H2646–H2652, 2008. First published April 11, 2008; doi:10.1152/ajpheart.00291.2008.—The sympathetic nervous system, via postganglionic innervation of blood vessels and the heart, is an important determinant of cardiovascular function. The mechanisms underlying sympathetic innervation of targets are not fully understood. This study tests the hypothesis that target-derived vascular endothelial growth factor (VEGF) promotes sympathetic innervation of blood vessels. Western blot and immunohistochemical analyses indicate that VEGF is produced by vascular cells in arteries and that VEGF receptors are expressed on sympathetic nerve fibers innervating arteries. In vitro, exogenously added VEGF and VEGF produced by vascular smooth muscle cells (VSMCs) in sympathetic neurovascular cocultures inhibited semaphorin 3A (Sema3A)-induced collapse of sympathetic growth cones. In the absence of Sema3A, VEGF and VSMCs also increased growth cone area. These effects were mediated via VEGF receptor 1. In vivo, the neutralization of VEGF inhibited the reinnervation of denervated femoral arteries. These data demonstrate that target-derived VEGF plays a previously unrecognized role in promoting the growth of sympathetic axons.

axon growth; sympathetic nervous system; vascular smooth muscle; vascular endothelial growth factor

THE SYMPATHETIC NERVOUS SYSTEM is a component of the autonomic nervous system that allows humans and other animals to respond to changes in their environment. In the cardiovascular system, the effects of the sympathetic nervous system are mediated via postganglionic sympathetic neurons innervating blood vessels and the heart. Vascular sympathetic innervation is an important determinant of blood pressure and blood flow, and alterations in vascular sympathetic innervation have been implicated in the development and maintenance of cardiovascular disease (6, 9, 17). Several lines of evidence suggest that the development and maintenance of sympathetic innervation are promoted at least in part by target-dependent mechanisms (7, 12, 18). However, these mechanisms are not completely understood.

Several lines of evidence suggest a role for VEGF and VEGF receptors in promoting and maintaining sympathetic innervation. VEGF is produced by sympathetic targets (4, 29, 32) and has been reported to stimulate sympathetic axon growth (8, 30). In addition, VEGF inhibits semaphorin 3A (Sema3A) binding to neuropilin-1 (NRP-1) (21, 23, 24). Sema3A binding to NRP-1 causes the collapse of sympathetic growth cones, acting as a repulsive directional signal for sympathetic axons (15, 16, 24). The VEGF inhibition of Sema3A binding suggests that VEGF would modulate sympathetic axon growth or guidance. VEGF mediates its actions via binding to three receptors: VEGF receptor 1 (VEGFR-1), VEGF receptor 2 (VEGFR-2), and NRP-1. Despite this evidence suggesting that VEGF and its receptors are likely to affect sympathetic target innervation, the expression and function of these molecules at sympathetic targets have not been studied.

The present study considers the role of VEGF as a determinant of vascular sympathetic innervation. In vitro and in vivo models are used to test the hypothesis that vascular-derived A isoform of VEGF ($VEGF_A$) promotes sympathetic axon growth at sympathetic neurovascular junctions. The roles of NRP-1, VEGFR-1, and VEGFR-2 are considered.

MATERIALS AND METHODS

Animals

The use of animals in the present studies was in accordance with the National Institutes of Health guidelines for the humane care and use of animals in research and was approved by the Institutional Animal Care and Use Committee of the University of Vermont.

Materials

Type I rat tail collagen (08-115) was from Upstate Biotechnology. Dulbecco's modified Eagle's medium (DMEM; 11885), DMEM/F12 (11320), fetal bovine serum (FBS; 16000-044), penicillin-streptomycin (15140-122), trypsin-EDTA (25300), and agarose (15510-027) were from GIBCO. NuSerum (355500) and mouse 2.5s nerve growth factor (NGF; 356004) were from BD Biosciences. Hyaluronidase (2592), collagenase (4176), and lyophilized trypsin (3707) were from Worthington Biotechnology. Bovine serum albumin (126609) and Triton X-100 (648463) were from Calbiochem. Recombinant rat $VEGF_{164}$ (564-RV), recombinant human Sema3A-Fc (1250-S3), NRP-1 antibody (AF566), VEGF-neutralizing antibody (AF564), VEGFR-1-neutralizing antibody (AF471), VEGFR-2-neutralizing antibody (AF644), normal goat IgG (AB-108-C), and normal rabbit IgG (AB-105-C) were from R&D Systems. Rabbit anti-growth associated protein 43 (GAP43; AB5220) antibody was from Chemicon. VEGF (SC-507), VEGFR-1 (SC-316), VEGFR-2 (SC-504), and goat anti-GAP43 (SC-7457) antibodies were from Santa Cruz. Mitomycin C (M4287), ethidium bromide (E1385), and antibodies to smooth muscle α-actin (A 2547) and tyrosine hydroxylase (TH; T 2928) were from Sigma. Evan's blue (206334) was from Aldrich. Isoflurane was from Webster Veterinary. PCR primers were from Integrated DNA Technologies. Alexa-Fluor fluorescent secondary antibodies were from Molecular Probes. Rabbit horseradish peroxidase (HRP)-conjugated secondary antibody (170-6515) was from Bio-Rad. Goat (31402) and mouse (1858143) HRP-conjugated secondary antibodies and Super Signal West Pico chemiluminescent substrate (34080) were from Pierce. RNeasy mini kit (74104), QIAshredder kit (79654), and QiaQuick gel extraction kit (28704) were from Qiagen. RetroScript kit (1710) was from Ambion. Amplitaq Gold (N808-0241) and deoxynucleotides (362275) were from Applied Biosystems. Tris-glycine

Address for reprint requests and other correspondence: D. Damon, Dept. of Pharmacology, Univ. of Vermont, 89 Beaumont Ave., Burlington, VT 05405 (e-mail: Deborah.Damon@uvm.edu).

The costs of publication of this article were defrayed in part by the payment of page charges. The article must therefore be hereby marked "*advertisement*" in accordance with 18 U.S.C. Section 1734 solely to indicate this fact.

SDS sample buffer (LC2676), 4–20% Tris-glycine polyacrylamide gels (EC6025BOX), Tris-acetate-EDTA buffer (15558-026), and Alexa-Fluor fluorescent secondary antibodies were from Invitrogen. Nitrocellulose membranes (10401196) were from Whatman. X-Omat Blue XB-1 film (1438795) was from Kodak. Osmotic minipumps (1002) were from Alzet. Prolene sutures (8695G) were from Ethicon [add in radioimmunoprecipitation assay (RIPA) buffer ingredients].

Tissue Culture

VSMCs were isolated from explants of adult postpartum Sprague-Dawley rat tail arteries (28). VSMCs were grown in DMEM supplemented with 10% FBS and 100 U/ml penicillin-streptomycin. VSMCs were used at *passage 1* for Western blot analyses and at *passage 2* for neurovascular cultures and immunocytochemical analyses.

Superior cervical ganglia were obtained from neonatal rats (2–4 days of age) and dissociated with collagenase-hyaluronidase digest followed by a trypsin digest. Cells were plated onto type I rat tail collagen-coated dishes (RT-PCR and Western blot analyses) or coverslips (immunohistochemistry). In cultures grown for >24 h, nonneuronal cells were growth arrested with mitomycin C (1 h, 10 μg/ml). All neuronal and neurovascular cultures were grown in neuronal growth medium (DMEM/F12 supplemented with 10% NuSerum, 5% FBS, 100 U/ml penicillin-streptomycin, and 50 ng/ml NGF).

Immunocytochemistry and Immunohistochemistry

Neuronal and neurovascular cultures were fixed with warm 4% formaldehyde in phosphate-buffered saline (PBS) for 12 min at room temperature. Arteries were fixed for 2 h using the same formaldehyde solution. Following fixation, the cells and arteries were transferred to PBS. The arteries were permeabilized for 9 min with 0.05% Triton X-100 in PBS, followed by two PBS washes. The cells and arteries were then incubated at room temperature for 20 min with 5% FBS in PBS to block nonspecific labeling, and the following primary antibodies were added and incubated overnight at 4°C: GAP43 (1 μg/ml), NRP-1 (2 μg/ml), VEGFR-1 (5 μg/ml, R&D Systems; and 2 μg/ml, Santa Cruz), and VEGFR-2 (5 μg/ml, R&D Systems; and 2 μg/ml, Santa Cruz). Unbound primary antibody was removed with three PBS washes. Samples were blocked for 5 min in 5% FBS in PBS, followed by incubation with corresponding secondary antibodies (Alexa-Fluor donkey anti-goat 647 and donkey anti-rabbit 555 or donkey anti-rabbit 647 and donkey anti-goat 546) for 1 h at room temperature. Four final PBS washes removed any unbound secondary antibody. Growth cones were visualized on an upright fluorescence microscope (Olympus BX50) with a ×60 oil objective. Images were recorded digitally with an Olympus camera (model U-ULH) and Magnafire software, analyzed with MetaMorph image analysis software, and viewed with Adobe Photoshop. Receptor immunocytochemistry and immunohistochemistry were visualized, digitally recorded, and adjusted with a Zeiss LSM510 Meta Laser Scanning Microscope and associated image capture software. IgG controls were used to eliminate the nonspecific signal. The camera gain was adjusted such that there was no detectable signal associated with the controls. This gain setting was then used to capture corresponding receptor images. Receptor antibody images and corresponding IgG control images were adjusted equivalently to ensure that the adjustment did not affect the interpretation of the data. The images were viewed in Adobe Photoshop.

Morphological Analyses

Growth cone collapse. For each sample, 100 growth cones were identified as collapsed or uncollapsed (see Fig. 3). The percent collapsed was thus equal to the number collapsed.

Growth cone area. The area of uncollapsed growth cones was measured using MetaMorph image analysis software. At least 20 uncollapsed growth cones were analyzed per sample. At least two independent samples were analyzed for each experimental condition.

Innervation density. Arteries were prepared for GAP43 immunofluorescence and visualized with an Olympus BX50 microscope using a ×10 objective. Images were recorded digitally with an Olympus camera (model U-ULH) and MagnaFire software and analyzed with MetaMorph image analysis software. The total length of GAP43 immunoreactive nerve fibers per unit area was determined. Two density measurements were made per artery and were averaged.

RT-PCR Analysis

RNA was isolated using RNeasy mini kits. The RNA was reverse transcribed using a RetroScript kit, and the cDNA was amplified using Amplitaq Gold. PCR reactions were carried out in an MJ Research PTC-200 Peltier thermal cycler under the following conditions: 95°C for 10 min, followed by 40 cycles of 94°C for 15 s, the appropriate annealing temperature for 30 s, and 72°C for 45 s. The final cycle was followed by a 10-min incubation at 72°C. PCR primers, annealing temperatures, and product sizes are shown in Table 1. PCR products were separated by 1.5% agarose gel electrophoresis in gels containing ethidium bromide and visualized with UV light. The amplified PCR products were isolated with a QIAquick gel extraction kit and sequenced by the University of Vermont DNA facility to confirm the identity of the DNA.

Western Blot Analysis

Tissues were excised from neonatal (9–11 days) and adult postpartum Sprague-Dawley rats and then lysed and homogenized in enhanced RIPA buffer containing 50 mM Tris base, 150 mM NaCl, 10 mM EDTA, 0.25% deoxycholate, 1% Nonidet P-40 substitute, 10% glycerol, 1% protease inhibitor cocktail, 1 mM DTT, and 0.1% sodium dodecyl sulfate. Cells were pelleted in PBS and then lysed in enhanced RIPA buffer. Samples were diluted with an equal volume of 2× electrophoresis loading buffer, boiled for 5 min, electrophoresed on 4–20% gradient Tris-glycine polyacrylamide gels, and transferred to nitrocellulose membranes. The membranes were blocked with 3% nonfat dry milk in PBS containing 0.05% Tween (PBST) for 20 min at room temperature and then incubated overnight at 4°C in blocking solution containing the appropriate primary antibody VEGF (1 μg/ml), VEGFR-1 (0.2 μg/ml), and VEGFR-2 (1 μg/ml; Santa Cruz); NRP-1 (0.1 μg/ml; R&D Systems); or TH (0.9 μg/ml) and smooth muscle α-actin (0.25 μg/ml; Sigma). Unbound primary antibody was removed with three 5-min washes with PBST. Blocking solution was applied for 10 min before incubation for 1 h at room temperature with the appropriate HRP-conjugated secondary antibody goat anti-rabbit

Table 1. *RT-PCR primers, annealing temperatures, and expected product sizes*

Gene	Sense, 5′-3′	Antisense, 5′-3′	Annealing Temperature, °C	Product Size, bp
VEGF	TCATGCGGATCAAACCTCACCAAA	TCACCGCCTTGGCTTGTCACAT	58	280
NRP-1	CGCCTGGTGAGCCCTGTGGTCTATT	TGTTCTTGTCGCCTTTCCCTTCTT	59	406
VEGFR1	CGGGCAAAGAATAGCGTGGGACAG	GGACAGCCGATGGGACCGTTTTC	60	529
VEGFR2	TCCCGTCCTCAAAGCATCAGCATA	GCAGGGGAGGGTTGGCATAGA	59	576

NRP-1, neuropilin-1; VEGFR-1 and VEGFR-2, VEGF receptor 1 and receptor 2, respectively.

(0.3 μg/ml; Bio-Rad) or goat anti-mouse (0.0025 μg/ml) and rabbit anti-goat (0.25 μg/ml; Pierce). The HRP was detected with Pierce Super Signal West Pico enhanced chemiluminescence and documented on autoradiographic film (Kodak X-Omat Blue XB-1).

In Vivo Denervation and Reinnervation

Adult postpartum Sprague-Dawley rats were anesthetized with a 3% solution of isoflurane on a Vet Equip Table Top Laboratory Animal Anesthesia System. The animal was placed in a supine position, and a small incision was made over the right, distal femoral area. The distal femoral artery was mechanically denervated by severing all connections to the femoral nerve. For VEGF reinnervation experiments, an Alzet model 1002 Micro-Osmotic Pump [containing 1% Evans blue and 10 μg VEGF neutralizing antibody (R&D Systems; specific to $VEGF_{164}$ and $VEGF_{120}$) or control IgG in PBS] was implanted subcutaneously adjacent to the denervated femoral arteries. The wound was closed using an Ethicon 6-0 prolene suture.

Four, seven, fourteen or twenty-one days postdenervation, denervated and contralateral control femoral arteries were harvested. The dispersal of the pump contents was verified by the distribution of Evans blue within the surgical area. Innervation densities were assessed, and percent reinnervation was determined (denervated innervation density/control innervation density × 100).

Statistical Analyses

Data are presented as means ± SE and were compared with one- or two-tailed unpaired *t*-tests, assuming unequal variances or one-way ANOVA. Differences were considered significant if P values were <0.05.

RESULTS

VEGF and VEGF Receptor Expression at Sympathetic Neurovascular Junctions

The overall hypothesis of this study is that VSMC-derived $VEGF_A$ promotes sympathetic axon growth. A corollary to this hypothesis is that VSMCs in innervated arteries produce $VEGF_A$ and the nerve terminals innervating the VSMCs have receptors for $VEGF_A$. Figure 1 shows easily detectable levels of VEGF mRNA (164 and 120 bp) and protein (42 kDa) in vitro in VSMCs and in vivo in neonatal and adult tail arteries ($n = 2$). Figure 2*A* shows that NRP-1, VEGFR-1, and VEGFR-2 mRNA and protein (NRP-1, 120; VEGFR-1, 130; and VEGFR-2, 150, 200, and 230 kDa) were expressed by dissociated, neonatal, and adult postganglionic sympathetic neurons ($n = 2$). Figure 2*B* shows immunocytochemical analyses of the expression of NRP-1, VEGFR-1, and VEGFR-2 in dissociated postganglionic sympathetic neurons. Corresponding GAP43 staining is shown to identify neuronal cells. Detectable levels of the three receptors were seen in both cell bodies and neurites ($n = 2$ to 3). Figure 2*C* shows in vivo immunohistochemical staining of NRP-1, VEGFR-1, and VEGFR-2 on the adventitial surface of neonatal and adult rat tail arteries ($n = 2$ to 3). Nerve fibers were positively identified by GAP43 staining. VEGFR-1, VEGFR-2, and NRP-1 were easily detected in nerve fibers on the surface of adult arteries. VEGFR-1 was also easily detected in nerve fibers on the surface of neonatal arteries, but the staining for VEGFR-2 and NRP-1 was difficult to distinguish from the underlying staining in the artery.

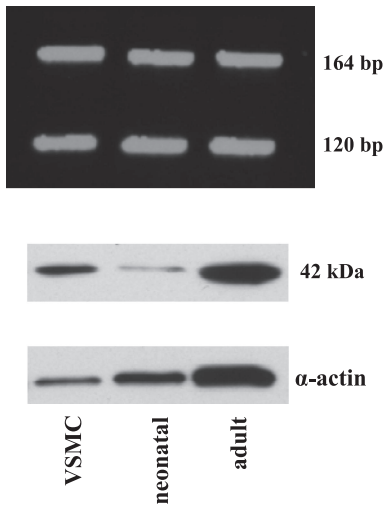

Fig. 1. Expression of vascular endothelial growth factor (VEGF) in innervated arteries. $VEGF_{164}$ expression in vascular smooth muscle cells (VSMCs) from adult rat tail artery in neonatal rat tail arteries and in adult rat tail arteries. Representative RT-PCR ($n = 2$ to 3 independent analyses) and Western blot ($n = 2$) analyses are shown. Corresponding smooth muscle α-actin Western blot analyses are shown to confirm that the samples contained VSMCs.

Vascular-derived VEGF and Sema 3A-induced Growth Cone Collapse

The studies of Miao et al. (21) and Narazaki and Giovanna (23) indicate that $VEGF_{164}$ and Sema3A compete for binding to NRP-1. It is known that Sema3A inhibits sympathetic axon growth via binding to NRP-1 (15, 16, 24). Thus $VEGF_{164}$ could affect axon growth by inhibiting Sema3A. To test this hypothesis, we evaluated the effects of exogenous and vascular-derived $VEGF_A$ on Sema3A-induced growth cone collapse. The effects of Sema3A (1 μg/ml for 1 h) were studied 1 day after plating and in the presence of 10 ng/ml NGF. The growth cone collapse data are shown in Fig. 3. Figure 3*A* shows representative collapsed and uncollapsed growth cones of dissociated postganglionic sympathetic neurons. Figure 3*B* shows the effects of exogenous $VEGF_{164}$ (1 μg/ml) on Sema3A-induced growth cone collapse. In these experiments, the VEGF was added with the Sema3A. These data indicate that Sema3A induced the collapse of growth cones in the cultures used in the present studies. Growth cone collapse in the presence of Sema3A (Fig. 3*B*, black bars) was greater than that in the absence of Sema3A (Fig. 3*B*, control, white bars; $P < 0.05$; unpaired *t*-test assuming unequal variance). These data also indicate that $VEGF_{164}$ reduced Sema3A-induced growth cone collapse ($P < 0.05$; unpaired *t*-test assuming unequal variances). $VEGF_{164}$ did not affect the percentage of growth cones that were collapsed in the absence of Sema3A ($P > 0.05$; unpaired *t*-test assuming unequal variances).

To determine whether vascular-derived $VEGF_A$ affected Sema3A-induced growth collapse, we assessed growth cone collapse in the presence of Sema3A (1 μg/ml for 1 h) in neuronal cultures that had been grown in the presence of VSMCs for 16–18 h (Fig. 3*C*). These experiments were performed in the presence of a control goat IgG (5 μg/ml) and in the presence of a goat antibody that neutralized the activity of $VEGF_A$ (5 μg/ml). In the presence of the control antibody, VSMCs decreased Sema3A-induced growth cone collapse ($P < 0.05$; unpaired *t*-test assuming unequal variances). This effect of VSMCs was blocked by the inhibition of VEGF.

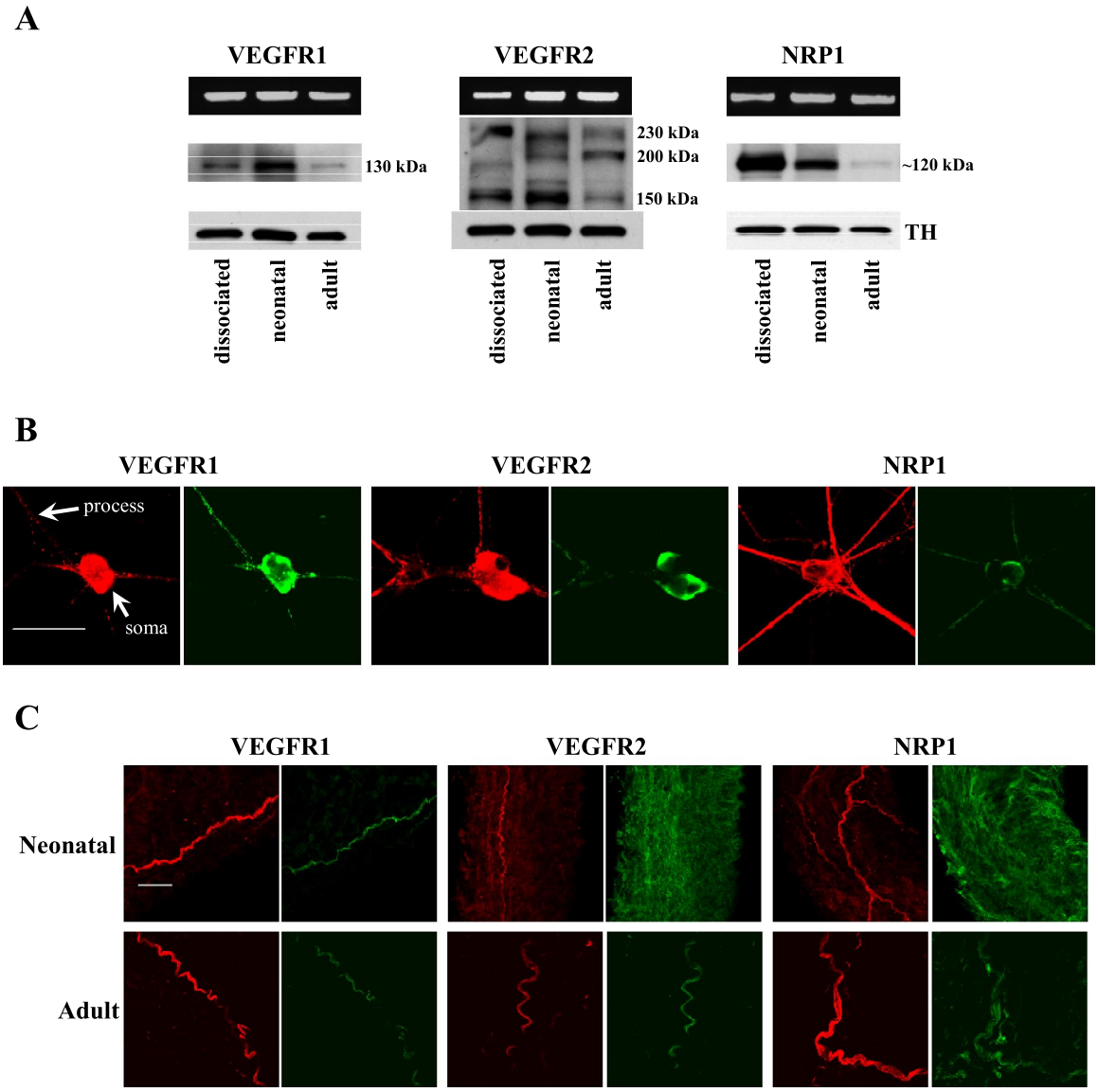

Fig. 2. Expression of VEGF receptors in postganglionic sympathetic neurons. *A*: representative RT-PCR ($n = 2$ independent analyses) and Western blot ($n = 2$) analyses of VEGF receptor gene expression in dissociated sympathetic neurons from neonatal rats (dissociated), in sympathetic ganglia from neonatal rats (neonatal), and in sympathetic ganglia from adult rats (adult). Corresponding tyrosine hydroxylase (TH) Western blot analyses are shown to confirm that the samples contained sympathetic neurons. Data for VEGF receptor 1 (VEGFR-1), VEGF receptor 2 (VEGFR-2), and neuropilin-1 (NRP-1) are shown. *B*: representative ($n \geq 2$) immunocytochemical analyses of VEGFR-1, VEGFR-2, and NRP-1 in dissociated sympathetic neurons from neonatal rats. *C*: representative ($n \geq 2$) immunohistochemical analyses of VEGFR-1, VEGFR-2, and NRP-1 in nerve fibers on the adventitial surface of neonatal and adult rat tail arteries. For *B* and *C*, VEGF receptor staining is shown in green (Alexa-Fluor 647) and GAP43 staining (to identify neurons and nerve fibers) is shown in red (Alexa-Fluor 555). VEGFR-1 and NRP-1 were detected with an antibody from R&D systems. VEGFR-2 was detected with an antibody from Santa Cruz Biotechnology and an antibody from R&D systems.

VSMCs did not affect the percentage of growth cones that were collapsed in the absence of Sema3A (data not shown).

Vascular-derived VEGF and Growth Cone Spreading

Although $VEGF_{164}$ and VSMCs did not affect the number of growth cones that were collapsed in the absence of Sema3A, these treatments did modulate the morphology of uncollapsed growth cones. Figure 4*A* shows representative images of uncollapsed growth cones of a sympathetic neuron grown in the absence of VSMCs and in a neuron grown for 16–18 h in the presence of VSMCs. Growth cones are labeled with GAP43 and shown in red. VSMCs are labeled with smooth muscle α-actin and shown in green. Figure 4*B* shows uncollapsed growth cone areas measured in control neurons and in neurons grown for 1 h in the presence of $VEGF_{164}$ or for 16–18 h in the presence of VSMCs. These data indicate that these treatments increased growth cone area [$P < 0.05$; nonparametric one-way ANOVA (Kruskal-Wallis) and Dunn's multiple comparisons]. Figure 4*C* shows that the effects of $VEGF_{164}$ and VSMCs on growth cone area are mediated by VEGFR-1. An antibody that prevented binding to VEGFR-1 completely inhibited the $VEGF_{164}$-induced increase in growth cone area and reduced the VSMC-induced increase [$P < 0.05$; nonparametric one-way ANOVA (Kruskal-Wallis) and Dunn's multiple comparisons]. Control antibody (IgG) and VEGFR-2 antibody were without effect.

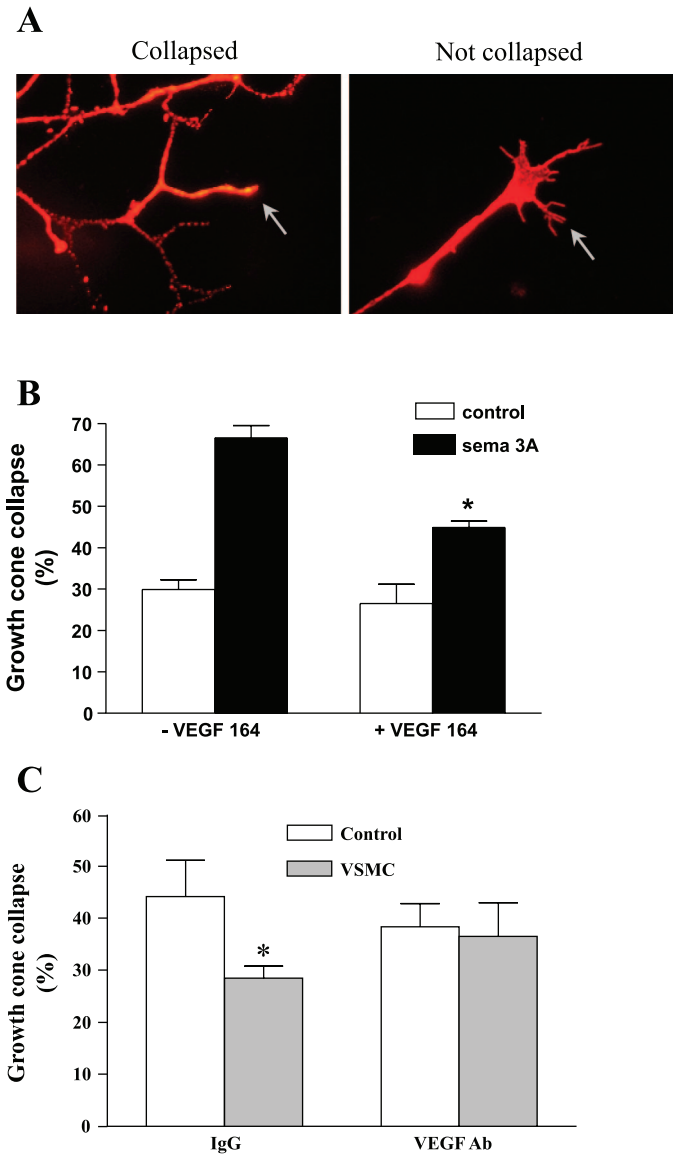

Fig. 3. Effects of VEGF on semaphorin 3A (Sema3A)-induced growth cone collapse. *A*: representative GAP43 immunohistochemistry showing collapsed vs. uncollapsed growth cones of dissociated neonatal postganglionic sympathetic neurons. Arrows point to growth cones. *B*: percentage of growth cones collapsed in neuronal cultures grown for 1 h in the absence (control; white bar) and presence (Sema3A; black bar) of 1 μg/ml Sema3A and in the absence and presence of 1 μg/ml $VEGF_{164}$. *Growth cone collapse in the presence of Sema3A plus $VEGF_{164}$ was less than that in the presence of Sema3A ($n \geq 4$ independent growth cones collapse assays; $P < 0.05$; two-tailed unpaired *t*-test assuming unequal variances). *C*: neurons were grown for 16–18 h in the absence (control; white bar) and presence (gray bar) of VSMCs. Percentage of growth cones collapsed in the presence of Sema3A (1 μg/ml for 1 h) was then determined. To assess the role of vascular-derived VEGF, experiments were performed in the presence of a control antibody (IgG) or in the presence of an antibody that neutralized the activity of VEGF (VEGF Ab). The antibodies were added at the time of neuronal plating. *Growth cone collapse in the presence of VSMCs was less than that in the absence of VSMCs ($n \geq 4$; $P < 0.05$; two-tailed unpaired *t*-test assuming unequal variances).

VEGF and Reinnervation of Denervated Femoral Arteries

Figures 1–4 indicate that $VEGF_A$ promotes sympathetic axon growth in vitro and thereby suggest that $VEGF_A$ would also promote sympathetic axon growth in vivo. To test this hypothesis, we assessed the effects of $VEGF_A$ on the reinnervation of denervated femoral arteries. Femoral arteries were mechanically denervated by severing the connections between the sympathetic nerve fibers on the artery and the femoral nerve. Figure 5*A* shows that this procedure resulted in almost complete denervation within 4 days and almost complete

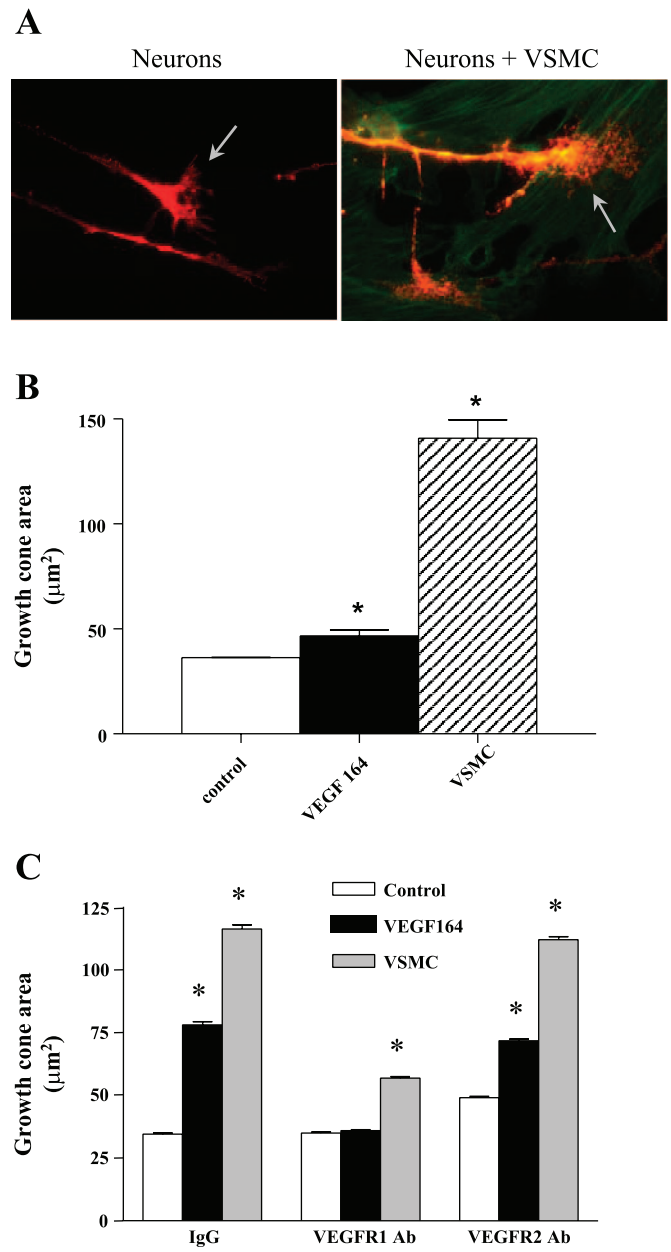

Fig. 4. Effects of VEGF on growth cone area. *A*: GAP43 (red) and smooth muscle α-actin (green) immunocytochemistry showing representative growth cones of neurons grown in the presence and absence of VSMCs. Arrows point to growth cones. *B*: growth cone areas of sympathetic neurons grown in the absence (control) and presence of $VEGF_{164}$ (1 μg/ml for 1 h) or VSMCs (16–18 h). *Treatments were significantly greater than those in control ($n \geq 96$ growth cones analyzed from ≥4 independent experiments; $P < 0.05$; Kruskal-Wallis nonparametric one-way ANOVA and Dunn's multiple comparison test). *C*: the effects of $VEGF_{164}$ (1 μg/ml for 1 h) and VSMCs (16–18 h) on growth cone area were assessed in the presence of control antibody (IgG), VEGFR-1 antibody (VEGFR-1 Ab), or VEGFR-2 Ab. The antibodies were added at the time of neuronal plating. *Significant differences from corresponding controls ($n \geq 20$ from ≥2 independent experiments; $P < 0.05$).

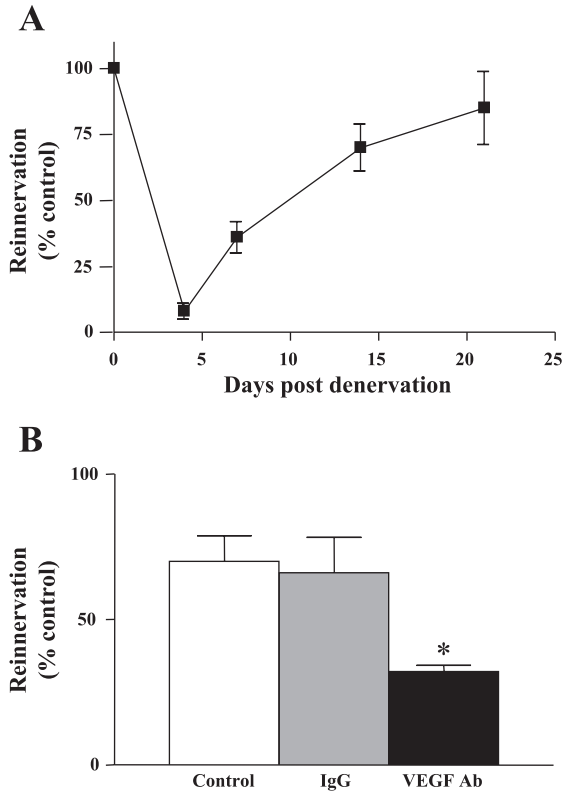

Fig. 5. VEGF and vascular reinnervation. *A*: time course of reinnervation following surgical denervation of femoral arteries. Data are presented as percentages of contralateral control ($n \geq 4$ animals). *B*: to determine the role of VEGF in femoral artery reinnervation, osmotic minipumps containing control antibody (IgG; 10 μg) or an antibody that neutralized the activity of VEGF (VEGF Ab; 10 μg) were implanted adjacent to denervated distal femoral arteries. Reinnervation was assessed as in *A* after 14 days. Control data are from *A*. *Statistically different from control ($n > 5$; $P < 0.05$; Kruskal-Wallis nonparametric one-way ANOVA with Dunn's multiple comparison test).

reinnervation within 21 days. Figure 5*B* shows that $VEGF_A$ promotes femoral artery reinnervation. Reinnervation after 14 days in the presence of an antibody that neutralized the activity of $VEGF_A$ was less than that in the absence of the antibody [$P < 0.05$; nonparametric one-way ANOVA (Kruskal-Wallis) and Dunn's multiple comparisons]. The control antibody was without effect.

DISCUSSION

VEGF is a pluripotent molecule that is best known for promoting vascularization and the growth of tumors (10, 25). Recent studies indicate that VEGF also has important implications for neuronal development, function, and disease (5, 14, 20, 26, 30, 31, 33, 35–37). Our results suggest a novel role for target-derived VEGF in promoting and/or maintaining the sympathetic innervation of blood vessels. Our in vitro studies suggest that VEGF produced by VSMCs affects sympathetic growth cones via two mechanisms. VEGF inhibits Sema3A-induced growth cone collapse, most likely by binding to NRP-1. VEGF also induces growth cone spreading via binding to VEGFR-1. Using an in vivo model, we further demonstrate that VEGF promotes the reinnervation of denervated femoral arteries.

The effects observed in the present study are consistent with previous reports that VEGF promotes sympathetic axon growth (8, 30) and indicate that VEGF also affects axon guidance. Increased growth cone area is associated with increased axon growth (19, 34). Thus the VEGF induction of growth cone spreading is likely to facilitate axon growth. VEGF inhibition of Sema3A-induced growth cone collapse would be permissive for axon growth, and thus VEGF could redirect the growth of axons. The neutralization of VEGF inhibited the reinnervation of denervated femoral arteries, suggesting that VEGF promoted the regrowth of axons or directed the growth of axons to the denervated femoral artery.

The reinnervation of denervated femoral arteries was inhibited by an antibody that neutralized the activities of $VEGF_{120}$ and $VEGF_{164}$. Our in vitro studies suggest that $VEGF_A$ may affect sympathetic axons via NRP-1 or VEGFR-1. Studies of Sondell et al. (30) suggest that $VEGF_A$ may stimulate axon growth via the activation of VEGFR-2. $VEGF_{120}$ and $VEGF_{164}$ mRNA and $VEGF_{164}$ protein were detected in arteries (Fig. 1), and NRP-1, VEGFR-1, and VEGFR-2 were detected in sympathetic fibers innervating arteries (Fig. 2). Thus it is likely that both VEGF isoforms and all three receptors facilitated reinnervation.

It should be noted that the observed effects of VEGF on vascular sympathetic innervation are likely to be mediated or modulated by the actions of other vascular-derived neuronal growth factors. In the present studies, the actions of VEGF were studied in the presence of NGF. Preliminary studies indicated that VEGF did not promote the survival of neonatal postganglionic sympathetic neurons grown in culture, and thus NGF was added (18). In vivo, sympathetic targets, including arteries, are known to produce NGF as well as VEGF (11, 27). Since NGF is known to promote the growth of sympathetic axons (11, 27), it is possible that the observed effects of VEGF were mediated or modulated by NGF. In addition, the data in Fig. 4 indicate that the growth cones of neurons grown in the presence of VSMCs were larger than those grown in the presence of VEGF. Correspondingly, an antibody that neutralized the activity of VEGFR-1 completely inhibited the VEGF-induced increase in growth cone area but only partially inhibited the VSMC-induced increase in growth cone area. These data indicate that a factor or factors other than VEGF contributed to the effect of VSMCs on growth cone area.

Mukouyama et al. (22) provided evidence that VEGF coordinates the growth of blood vessels and sensory innervation, whereas Bearden and Segal (1) demonstrated that vascular-derived VEGF coordinated the regrowth of motor neurons. The present studies demonstrate that vascular-derived VEGF coordinates the sympathetic reinnervation of blood vessels and thus provide further evidence that one of the key functions of VEGF is to coordinate the development of nerves and blood vessels (5). It is also likely that the observed effects of VEGF on sympathetic innervation are of clinical significance. This increased innervation is thought to contribute to the development and maintenance of hypertension (6, 9, 17). Cardiac sympathetic innervation is lost following myocardial infarction (13) and cardiac transplantation (2, 3). Reinnervation is limited, but when it occurs, it improves cardiac function (2, 13). The present studies provide new insight into the mechanisms that promote sympathetic innervation to blood vessels. This insight

may suggest novel therapeutic approaches for promoting reinnervation or inhibiting hyperinnervation.

GRANTS

This work was supported by the National Heart, Lung, and Blood Institute Grants HL-68009 and HL-076774 (to D. H. Damon).

REFERENCES

1. **Bearden SE, Segal SS.** Microvessels promote motor nerve survival and regeneration through local VEGF release following ectopic reattachment. *Microcirculation* 11: 633–644, 2004.
2. **Bengel FM, Ueberfuhr P, Schiepel N, Nekolla SG, Reichart B, Schwaiger M.** Effect of sympathetic reinnervation on cardiac performance after heart transplantation. *N Engl J Med* 345: 731–738, 2001.
3. **Bengel FM, Ueberfuhr P, Hesse T, Schiepel N, Ziegler SI, Scholz S, Nekolla SG, Reichart B, Schwaiger M.** Clinical determinants of ventricular sympathetic reinnervation after orthotopic heart transplantation. *Circulation* 106: 831–835, 2002.
4. **Burt LE, Forbes MS, Thornhill BA, Kiley SC, Chevalier RL.** Renal vascular endothelial growth factor in neonatal obstructive nephropathy. II. Endogenous VEGF. *Am J Physiol Renal Physiol* 292: F158–F167, 2007.
5. **Carmeliet P, Tessier-Lavigne M.** Common mechanisms of nerve and blood vessel wiring. *Nature* 436: 193–200, 2005.
6. **Clark DWJ.** Effects of immunosympathectomy on development of high blood pressure in genetically hypertensive rats. *Circ Res* 28: 330–336, 1971.
7. **Damon DH, teRiele JA, Marko SB.** Vascular-derived artemin: a determinant of vascular sympathetic innervation? *Am J Physiol Heart Circ Physiol* 293: H266–H273, 2007.
8. **Damon DH.** Vascular endothelial-derived semaphorin 3 inhibits sympathetic axon growth. *Am J Physiol Heart Circ Physiol* 290: H1220–H1225, 2006.
9. **Dhítal KK, Gerli R, Lincoln J, Milner P, Tanganelli P, Weber G, Fruschelli C, Burnstock G.** Increased density of perivascular nerves to the major cerebral vessels of the spontaneously hypertensive rat: differential changes in noradrenaline and neuropeptide Y during development. *Brain Res* 444: 33–45, 1988.
10. **Ferrara N, Gerber HP, LeCouter J.** The biology of VEGF and its receptors. *Nat Med* 9: 669–676, 2003.
11. **Glebova NO, Ginty DD.** Growth and survival signals controlling sympathetic nervous system development. *Annu Rev Neurosci* 28: 191–222, 2005.
12. **Glebova NO, Ginty DD.** Heterogeneous requirement of NGF for sympathetic target innervation in vivo. *J Neurosci* 24: 743–751, 2004.
13. **Hartikainen J, Kuikka J, Mantysaari M, Lansimies E, Pyoralak K.** Sympathetic reinnervation after acute myocardial infarction. *Am J Cardiol* 77: 5–9, 1996.
14. **Jin K, Mao XO, Greenberg DA.** Vascular endothelial growth factor stimulates neurite outgrowth from cerebral cortical neurons via Rho kinase signaling. *J Neurobiol* 66: 236–242, 2006.
15. **Kawasaki T, Bekku Y, Suto F, Kitsukawa T, Taniguchi M, Nagatsu I, Nagatsu T, Itoh K, Yagi T, Fujisawa H.** Requirement of neuropilin 1-mediated Sema3A signals in patterning of the sympathetic nervous system. *Develop* 129: 671–680, 2002.
16. **Kolodkin AL, Levengood DV, Rowe EG, Tai YT, Giger RJ, Ginty DD.** Neuropilin is a semaphorin III receptor. *Cell* 90: 753–762, 1997.
17. **Lee RM, Triggle CR, Cheung DWT, Coughlin MD.** Structural and functional consequences of neonatal sympathectomy on the blood vessels of spontaneously hypertensive rats. *Hypertens* 10: 328–338, 1987.
18. **Levi-Montalcini R, Booker B.** Destruction of the sympathetic ganglia in mammals by an antiserum to the nerve growth-promoting factor. *Proc Natl Acad Sci USA* 46: 384–391, 1960.
19. **Marquardt T, Shirasaki R, Ghosh S, Andrews SE, Carter N, Hunter T, Pfaff SL.** Coexpressed EphA receptors and Ephrin-A ligands mediate opposing actions on growth cone navigation from distinct membrane domains. *Cell* 121: 127–139, 2005.
20. **McCloskey DP, Croll SD, Scharfman HD.** Depression of synaptic transmission by vascular endothelial growth factor in adult rat hippocampus and evidence for increased efficacy after chronic seizures. *J Neurosci* 25: 8889–8897, 2005.
21. **Miao HQ, Soker S, Feiner L, Alonso JL, Raper JA, Klagsbrun M.** Neuropilin-1 mediates collapsin-1/semaphorin III inhibition of endothelial cell motility: functional competition of collapsin-1 and vascular endothelial growth factor-165. *J Cell Biol* 146: 233–241, 1999.
22. **Mukouyama YS, Shin D, Britsch S, Taniguchi M, Anderson DJ.** Sensory nerves determine the pattern of arterial differentiation and blood vessel branching in the skin. *Cell* 109: 693–705, 2002.
23. **Narazaki M, Giovanna T.** Ligand-induced internalization selects use of common receptor neuropilin-1 by VEGF165 and semaphorin3A. *Blood* 107: 3892–3901, 2006.
24. **Neufeld G, Cohen T, Shraga N, Lange T, Kessler O, Herzog Y.** The neuropilins: multifunctional semaphorin and VEGF receptors that modulate axon guidance and angiogenesis. *TCM* 12: 13–19, 2002.
25. **Neufeld G, Cohen T, Gengrinovitch S, Poltorak Z.** Vascular endothelial growth factor (VEGF) and its receptors. *FASEB J* 13: 9–22, 1999.
26. **Nishijima K, Ng YS, Zhong L, Bradley J, Schubert W, Jo N, Akita J, Samuelsson SJ, Robinson GS, Adamis AP, Shima DT.** Vascular endothelial growth factor-A is a survival factor for retinal neurons and a critical neuroprotectant during the adaptive response to ischemic injury. *Am J Pathol* 171: 53–67, 2007.
27. **O′Keeffe GW, Gutierrez H, Pandolfi PP, Riccardi C, Davies AM.** NGF-promoted axon growth and target innervation requires GITRL-GITR signaling. *Nat Neurosci* 11: 135–142, 2008.
28. **Ross R.** The smooth muscle cell. II. Growth of smooth muscle in culture and formation of elastic fibers. *J Cell Biol* 50: 172–186, 1971.
29. **Shimojo N, Jesmin S, Zaedi S, Otsuki T, Maeda S, Yamaguchi N, Aonuma K, Hattori Y, Miyauchi T.** Contributory role of VEGF overexpression in endothelin-1-induced cardiomyocyte hypertrophy. *Am J Physiol Heart Circ Physiol* 293: H474–H481, 2007.
30. **Sondell M, Sundler F, Kanje M.** Vascular endothelial growth factor is a neurotrophic factor which stimulates axonal outgrowth through the flk-1 receptor. *Eur J Neurosci* 12: 4243–4254, 2000.
31. **Storkebaum E, Lambrechts D, Dewerchin M, Moreno-Murciano MP, Appelmans S, Oh H, Van Damme P, Rutten B, Man WY, De Mol M, Wyns S, Manka D, Vermeulen K, Van Den Bosch L, Mertens N, Schmitz C, Robberecht W, Conway EM, Collen D, Moons L, Carmeliet P.** Treatment of motoneuron degeneration by intracerebroventricular delivery of VEGF in a rat model of ALS. *Nat Neurosci* 8: 85–92, 2005.
32. **Tischer E, Mitchell R, Hartman T, Silva M, Gospodarowicz D, Fiddes JC, Abraham JA.** The human gene for vascular endothelial growth factor. *J Biol Chem* 266: 11947–11954, 1991.
33. **Tovar-y-Romo LB, Zepeda A, Tapia R.** Vascular endothelial growth factor prevents paralysis and motoneuron death in a rat model of excitotoxic spinal cord neurodegeneration. *J Neuropathol Exp Neurol* 66: 913–922, 2007.
34. **Valerio A, Ghisi V, Dossena M, Tonello C, Giordano A, Frontini A, Ferrario M, Pizzi M, Spano P, Carruba MO, Nisoli E.** Leptin increases axonal growth cone size in developing mouse cortical neurons by convergent signals inactivating glycogen synthase kinase-3β. *J Biol Chem* 281: 12950–12958, 2006.
35. **Wang Y, Ou Mao X, Xie L, Banwait S, Marti HH, Greenberg DA, Jin K.** Vascular endothelial growth factor overexpression delays neurodegeneration and prolongs survival in amyotrophic lateral sclerosis mice. *J Neurosci* 27: 304–307, 2007.
36. **Warner-Schmidt JL, Duman RS.** VEGF is an essential mediator of the neurogenic and behavioral actions of antidepressants. *Proc Natl Acad Sci USA* 104: 4647–4652, 2007.
37. **Yasuhara T, Shingo T, Date I.** The potential role of vascular endothelial growth factor in the central nervous system. *Rev Neurosci* 15: 293–307, 2004.